



## Do Neocortical Pyramidal Neurons Display Stochastic Resonance?

MICHAEL RUDOLPH AND ALAIN DESTEXHE

*Unité de Neurosciences Intégratives et Computationnelles, CNRS, Bat. 33, Avenue de la Terrasse 1, 91198 Gif-sur-Yvette, France; Department of Physiology, Laval University, Québec G1K 7P4, Canada*

Michael.Rudolph@iaf.cnrs-gif.fr

Alain.Destexhe@iaf.cnrs-gif.fr

*Received June 22, 2000; Revised March 30, 2001; Accepted April 2, 2001*

Action Editor: Dr. E. Fetz

**Abstract.** Neocortical pyramidal neurons in vivo are subject to an intense synaptic background activity that has a significant impact on various electrophysiological properties and dendritic integration. Using detailed biophysical models of a morphologically reconstructed neocortical pyramidal neuron, in which synaptic background activity was simulated according to recent measurements in cat parietal cortex in vivo, we show that the responsiveness of the cell to additional periodic subthreshold stimuli can be significantly enhanced through mechanisms similar to stochastic resonance. We compare several paradigms leading to stochastic resonance-like behavior, such as varying the strength or the correlation in the background activity. A new type of resonance-like behavior was obtained when the correlation was varied, in which case the responsiveness is sensitive to the statistics rather than the strength of the noise. We suggest that this type of resonance may be relevant to information processing in the cerebral cortex.

**Keywords:** cerebral cortex, synaptic background activity, neocortex, noise, computational models

### 1. Introduction

Over the last two decades, phenomena like the amplification of weak signals or the improvement of signal detection and reliability of information transfer in nonlinear dynamical systems in the presence of a certain nonzero noise level were subject of an increasing number of theoretical and experimental investigations. They became well known and are now well established under the term *stochastic resonance* (SR). Since its first appearance as a possible explanation of the periodicity of Earth's ice ages (Benzi et al., 1981; Nicolis, 1982), SR has shown to be an inherit property of many physical, chemical and biological systems. For a comprehensive review and up-to-date summary of the basic theoretical principles underlying SR, experimental verifications, and applications,

we refer to Gammaitoni et al. (1998) and references therein.

Neurons provide particularly favorable conditions for displaying SR—namely, they are strongly excitable and nonlinear, and often they are subject to noisy environments. Indeed, evidence for SR was found in neurons, both theoretically (e.g., Bezrukov and Vodyanoy, 1997; Bulsara et al., 1991; Capurro et al., 1998; Chow et al., 1998; Huber et al., 1998; Lee et al., 1998; Lee and Kim, 1999; Longtin, 1993; Longtin and Chialvo, 1998; Mar et al., 1999; Mato, 1998; Neiman et al., 1999a, 1999b; Shimokawa et al., 1999; Wang et al., 1998; Wiesenfeld and Moss, 1995) and experimentally (e.g., Chialvo and Apkarian, 1993; Collins et al., 1995, 1996; Denk and Webb, 1989; Douglas et al., 1993; Ivey et al., 1998; Jaramillo and Wiesenfeld, 1998; Levin and Miller, 1996; Pei et al., 1996; Richardson et al.,



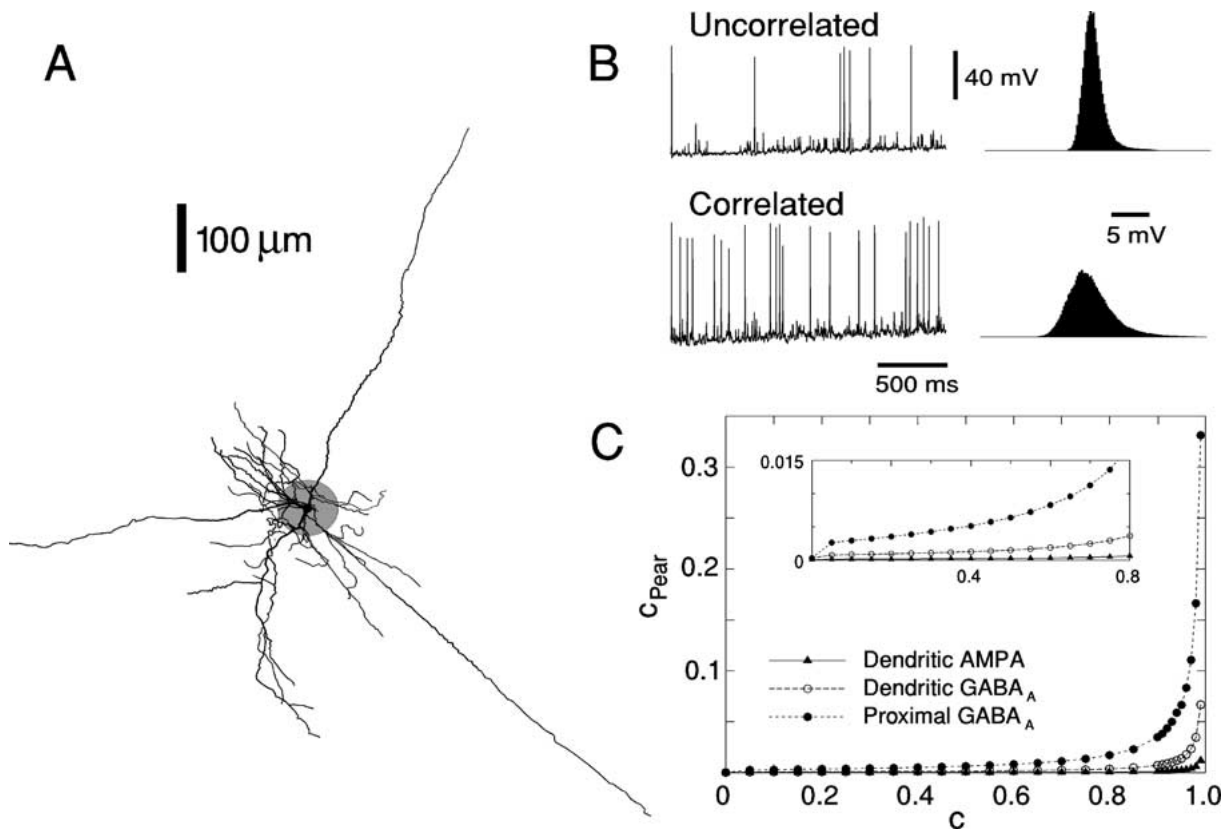


Figure 1. Morphology and electrophysiology of a neuron.

Panel A: Morphological reconstruction of a neuron. Scale bar: 100  $\mu\text{m}$ .

Panel B: Membrane potential ( $V_m$ ) traces showing uncorrelated and correlated firing patterns. Scale bars: 40 mV, 5 mV, 500 ms.

Panel C: Scatter plot of  $C_{Pear}$  vs  $C$  for three conditions: Dendritic AMPA (filled triangles), Dendritic  $GABA_A$  (open circles), and Proximal  $GABA_A$  (filled circles). The inset shows a zoomed-in view of the region where  $C$  is between 0.4 and 0.8 and  $C_{Pear}$  is between 0 and 0.015.

$I_{CL}$  (Llinás 1992;

1988)  $\approx 0.5 \text{ nA}$   $\approx 0.5 \text{ nA}$   $\approx 0.5 \text{ nA}$

1990; (Llinás 1992; (Llinás

1992; (Llinás 1992; (Llinás

1992; (Llinás 1992; (Llinás

1992; (Llinás 1992; (Llinás

1992; (Llinás 1992; (Llinás

1992; (Llinás 1992; (Llinás

1992; (Llinás 1992; (Llinás

1992; (Llinás 1992; (Llinás

1992; (Llinás 1992; (Llinás

1992; (Llinás 1992; (Llinás

1992; (Llinás 1992; (Llinás

1992; (Llinás 1992; (Llinás

1992; (Llinás 1992; (Llinás

1992; (Llinás 1992; (Llinás

1992; (Llinás 1992; (Llinás

(DeFelice 1992; (DeFelice 1991; (DeFelice

1989),  $g_{GABA} = 6,563 \text{ pS}$

$g_{GABA_A} = 3,376 \text{ pS}$   $g_{GABA_A} = 2,818 \text{ pS}$

$g_{GABA} = 558 \text{ pS}$   $g_{GABA} = 558 \text{ pS}$

$g_{GABA} = 558 \text{ pS}$   $g_{GABA} = 558 \text{ pS}$

$g_{GABA} = 558 \text{ pS}$   $g_{GABA} = 558 \text{ pS}$

$g_{GABA} = 558 \text{ pS}$   $g_{GABA} = 558 \text{ pS}$

$g_{GABA} = 558 \text{ pS}$   $g_{GABA} = 558 \text{ pS}$

$g_{GABA} = 558 \text{ pS}$   $g_{GABA} = 558 \text{ pS}$

$g_{GABA} = 558 \text{ pS}$   $g_{GABA} = 558 \text{ pS}$

$g_{GABA} = 558 \text{ pS}$   $g_{GABA} = 558 \text{ pS}$

$g_{GABA} = 558 \text{ pS}$   $g_{GABA} = 558 \text{ pS}$

$g_{GABA} = 558 \text{ pS}$   $g_{GABA} = 558 \text{ pS}$

$g_{GABA} = 558 \text{ pS}$   $g_{GABA} = 558 \text{ pS}$

$g_{GABA} = 558 \text{ pS}$   $g_{GABA} = 558 \text{ pS}$

$g_{GABA} = 558 \text{ pS}$   $g_{GABA} = 558 \text{ pS}$

$g_{GABA} = 558 \text{ pS}$   $g_{GABA} = 558 \text{ pS}$

(DeFelice 1999; (DeFelice 1998), (DeFelice

1999)

Table 2. Parameters of the model neurons.

Parameter	Value	Units
$E_N$	50	mV
$E_K$	-90	mV
$\bar{g}_{Na}$	$a_c \cdot 516$	$\mu S \cdot m^2$
$\bar{g}_{Kd}$	$a_c \cdot 100$	$\mu S \cdot m^2$
$\bar{g}_{Ks}$	$a_c \cdot 51.6$	$\mu S \cdot m^2$
$\bar{g}_{Ca}$	$a_c \cdot 10$	$\mu S \cdot m^2$
$\bar{g}_{Cl}$	$a_c \cdot 74.8$	$\mu S \cdot m^2$
$\bar{g}_{Mg}$	$a_c \cdot 14.5$	$\mu S \cdot m^2$
$\bar{g}_{Mn}$	$a_c \cdot 0.5$	$\mu S \cdot m^2$
$\bar{g}_{Mg}$	$a_c \cdot 0.725$	$\mu S \cdot m^2$

Table 3. Parameters of the model synapses.

Parameter	Value	Units
$\alpha_{BAA}$	$5 \text{ s}^{-1} \text{ M}^{-1}$	$\text{M}^{-1}$
$\alpha_{AR}$	$1.1 \text{ s}^{-1} \text{ M}^{-1}$	$\text{M}^{-1}$
$\alpha_{ARin}$	$1.1 \text{ s}^{-1} \text{ M}^{-1}$	$\text{M}^{-1}$
$\beta_{BAA}$	$0.1 \text{ s}^{-1}$	$\text{s}^{-1}$
$\beta_{AR}$	$0.67 \text{ s}^{-1}$	$\text{s}^{-1}$
$\beta_{ARin}$	$0.19 \text{ s}^{-1}$	$\text{s}^{-1}$
$C_{maxBAA}$	1	M
$C_{maxAR}$	1	M
$C_{maxARin}$	1	M
$C_{durBAA}$	1	s
$C_{durAR}$	1	s
$C_{durARin}$	1	s
$E_{revBAA}$	-75	mV
$E_{revAR}$	0	mV
$E_{revARin}$	0	mV
$E_{prethresARin}$	0	mV
$T_{deadARin}$	1	s
$g_{BAA}$	$a_s \cdot 869.4$	$\mu S$
$g_{AR}$	$a_s \cdot 1738.8$	$\mu S$
$g_{ARin}$	0.1	$\mu S \cdot m^{-2}$
$N_{BAA}$	2818	
$N_{AR}$	16563	
$N_{ARin}$	197	

The model consists of a population of  $N_0$  neurons, each with a set of ion channels and synapses. The parameters of the model are listed in Tables 2 and 3. The model is simulated using a standard numerical method (e.g., Runge-Kutta). The results of the simulation are shown in Figure 1. The model shows a transition from a stable state to a state with large, irregular oscillations as the coupling strength  $c$  is increased. This transition is characterized by a bifurcation diagram (Fig. 1C) showing a period-doubling cascade. The critical coupling strength  $c_c$  is approximately 0.197. For  $c > c_c$ , the system exhibits chaotic behavior. The model is implemented in C++ and is available as open-source software.

The model is based on the integrate-and-fire neuron model (Destexhe et al., 1999). The neuron membrane potential  $V_m$  is governed by the following equation:

$$C \dot{V}_m = -I_{leak} - I_{Na} - I_{Kd} - I_{Ks} - I_{Ca} - I_{Mg} - I_{Mn} + I_{syn}$$

where  $C$  is the membrane capacitance,  $I_{leak}$  is the leak current,  $I_{Na}$ ,  $I_{Kd}$ ,  $I_{Ks}$ ,  $I_{Ca}$ ,  $I_{Mg}$ , and  $I_{Mn}$  are the currents carried by the different ion channels, and  $I_{syn}$  is the synaptic current. The synaptic current is given by:

$$I_{syn} = \sum_j g_{syn} (V_m - E_{syn}) s_j$$

where  $g_{syn}$  is the synaptic conductance,  $V_m$  is the membrane potential,  $E_{syn}$  is the reversal potential, and  $s_j$  is the synaptic variable. The synaptic variable  $s_j$  is governed by the following equation:

$$\dot{s}_j = -\beta s_j + \alpha [V_m - E_{prethres} - T_{dead}]^n$$

where  $\beta$  is the synaptic decay time constant,  $\alpha$  is the synaptic activation time constant,  $E_{prethres}$  is the presynaptic threshold, and  $T_{dead}$  is the synaptic dead time. The model is simulated using a standard numerical method (e.g., Runge-Kutta). The results of the simulation are shown in Figure 1. The model shows a transition from a stable state to a state with large, irregular oscillations as the coupling strength  $c$  is increased. This transition is characterized by a bifurcation diagram (Fig. 1C) showing a period-doubling cascade. The critical coupling strength  $c_c$  is approximately 0.197. For  $c > c_c$ , the system exhibits chaotic behavior. The model is implemented in C++ and is available as open-source software.

The first part of the paper discusses the importance of the time constant  $T_{in}$  in the analysis of the system response. The second part of the paper discusses the importance of the time constant  $T_{in}$  in the analysis of the system response. The third part of the paper discusses the importance of the time constant  $T_{in}$  in the analysis of the system response.

2.2. Data Analysis and Measures of Response Coherence

The first part of the paper discusses the importance of the time constant  $T_{in}$  in the analysis of the system response. The second part of the paper discusses the importance of the time constant  $T_{in}$  in the analysis of the system response. The third part of the paper discusses the importance of the time constant  $T_{in}$  in the analysis of the system response.

(Dinh 2000).

$$19 = 524,288$$

2.2.1. Power Spectral Analysis.

The first part of the paper discusses the importance of the time constant  $T_{in}$  in the analysis of the system response. The second part of the paper discusses the importance of the time constant  $T_{in}$  in the analysis of the system response. The third part of the paper discusses the importance of the time constant  $T_{in}$  in the analysis of the system response.

The first part of the paper discusses the importance of the time constant  $T_{in}$  in the analysis of the system response. The second part of the paper discusses the importance of the time constant  $T_{in}$  in the analysis of the system response. The third part of the paper discusses the importance of the time constant  $T_{in}$  in the analysis of the system response.

2.2.2. ISI Distribution.

The first part of the paper discusses the importance of the time constant  $T_{in}$  in the analysis of the system response. The second part of the paper discusses the importance of the time constant  $T_{in}$  in the analysis of the system response. The third part of the paper discusses the importance of the time constant  $T_{in}$  in the analysis of the system response.

As such, the “ $\tau$ ” represents the time constant of the membrane time constant.

$$D_i = \frac{N_b \cdot i}{N_b \times T_b} \sim \frac{N_b \cdot i}{T_b} \quad (2)$$

El  $N_b \cdot i$  represents the total number of spikes,  $T_b$  is the total time, and  $T_b$  is the total time.  $N_b$  is the number of spikes,  $T_b$  is the total time, and  $T_b$  is the total time.

2.2.3. Coherence Between Output and Stimulus.

As such, the coherence between output and stimulus is defined as (Chapman 1993):

$$CS_i = \frac{N_b \cdot i}{N_b} \quad (3)$$

As such, the coherence between output and stimulus is defined as (Chapman 1993):

2.2.4. Probability for Evoking Spikes.

As such, the probability for evoking spikes is defined as (Chapman 1993):

$$P_p = \frac{N_p}{N_b} \quad (4)$$

As such, the probability for evoking spikes is defined as (Chapman 1993):

As such, the probability for evoking spikes is defined as (Chapman 1993):

$$N^* = \frac{P_p}{\sigma_v} \quad (5)$$

As such, the probability for evoking spikes is defined as (Chapman 1993):

3. Results

As such, the probability for evoking spikes is defined as (Chapman 1993):



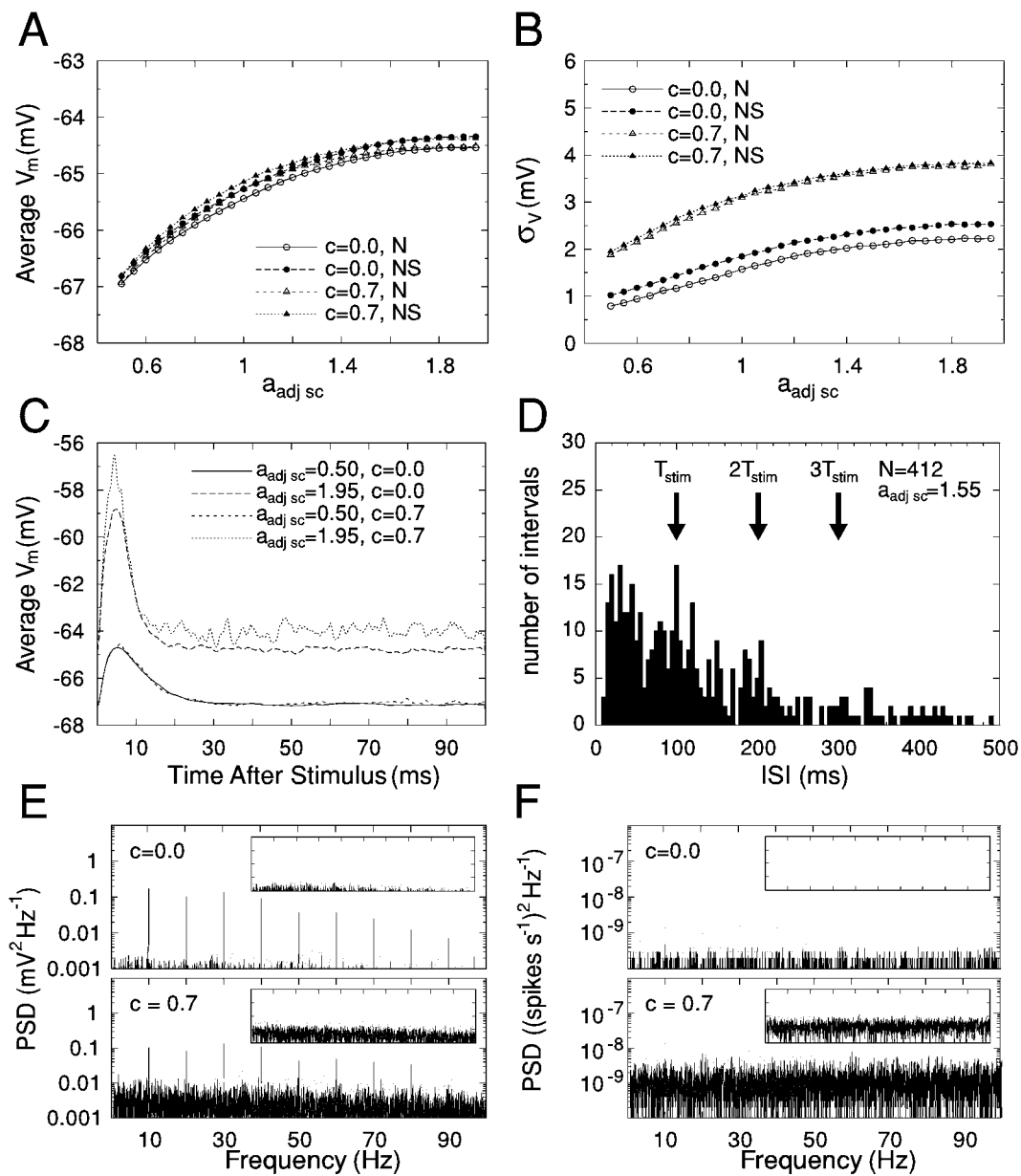


Figure 2. Bursting in the

Figure 2. Bursting in the  $V_m$  (A) and its variability  $\sigma_V$  (B) as a function of the adjusted synaptic conductance  $a_{adj\ sc}$  for different values of the coupling constant  $c$  (0.0 and 0.7) and the noise level (N and NS). Panel C shows the time course of the average membrane potential  $V_m$  after a stimulus for different values of  $a_{adj\ sc}$  and  $c$ . Panel D is a histogram of the interspike intervals (ISI) for  $N=412$  trials with  $a_{adj\ sc}=1.55$  and  $T_{stim}=100$  ms. Panel E and F show the power spectral density (PSD) of the membrane potential for  $c=0.0$  and  $c=0.7$ , respectively, on a linear (E) and logarithmic (F) scale.





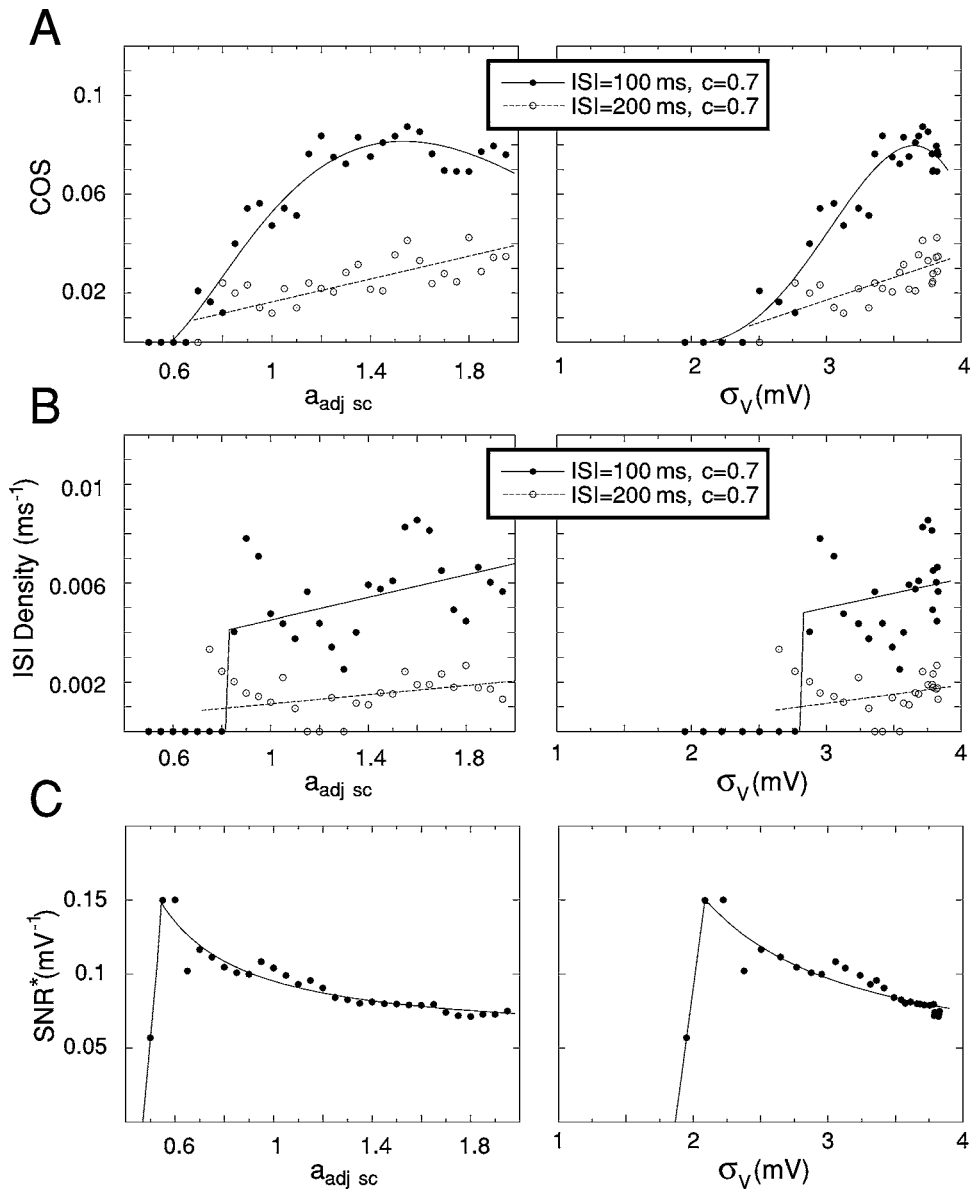


Figure 3. Characteristic curves of the model for  $c = 0.7$ . The left column shows the relationship between the adjusted synaptic conductance  $a_{adj\ sc}$  and the metrics COS, ISI Density, and SNR\*. The right column shows the relationship between the standard deviation of the synaptic conductance  $\sigma_V$  and the same metrics. The top row (A) shows COS, the middle row (B) shows ISI Density ( $ms^{-1}$ ), and the bottom row (C) shows SNR\* ( $mV^{-1}$ ). Filled circles and solid lines represent  $ISI = 100\ ms, c = 0.7$ . Open circles and dashed lines represent  $ISI = 200\ ms, c = 0.7$ .

Figure 3. Characteristic curves of the model for  $c = 0.7$ . The left column shows the relationship between the adjusted synaptic conductance  $a_{adj\ sc}$  and the metrics COS, ISI Density, and SNR\*. The right column shows the relationship between the standard deviation of the synaptic conductance  $\sigma_V$  and the same metrics. The top row (A) shows COS, the middle row (B) shows ISI Density ( $ms^{-1}$ ), and the bottom row (C) shows SNR\* ( $mV^{-1}$ ). Filled circles and solid lines represent  $ISI = 100\ ms, c = 0.7$ . Open circles and dashed lines represent  $ISI = 200\ ms, c = 0.7$ .

's

Figure 3. Characteristic curves of the model for  $c = 0.7$ . The left column shows the relationship between the adjusted synaptic conductance  $a_{adj\ sc}$  and the metrics COS, ISI Density, and SNR\*. The right column shows the relationship between the standard deviation of the synaptic conductance  $\sigma_V$  and the same metrics. The top row (A) shows COS, the middle row (B) shows ISI Density ( $ms^{-1}$ ), and the bottom row (C) shows SNR\* ( $mV^{-1}$ ). Filled circles and solid lines represent  $ISI = 100\ ms, c = 0.7$ . Open circles and dashed lines represent  $ISI = 200\ ms, c = 0.7$ .

Figure 3. Characteristic curves of the model for  $c = 0.7$ . The left column shows the relationship between the adjusted synaptic conductance  $a_{adj\ sc}$  and the metrics COS, ISI Density, and SNR\*. The right column shows the relationship between the standard deviation of the synaptic conductance  $\sigma_V$  and the same metrics. The top row (A) shows COS, the middle row (B) shows ISI Density ( $ms^{-1}$ ), and the bottom row (C) shows SNR\* ( $mV^{-1}$ ). Filled circles and solid lines represent  $ISI = 100\ ms, c = 0.7$ . Open circles and dashed lines represent  $ISI = 200\ ms, c = 0.7$ .

$a_{adj\ sc}$

$\sigma_V$

A: Ch

B: ISI

C: SNR\*

\*

Figure 3. Characteristic curves of the model for  $c = 0.7$ . The left column shows the relationship between the adjusted synaptic conductance  $a_{adj\ sc}$  and the metrics COS, ISI Density, and SNR\*. The right column shows the relationship between the standard deviation of the synaptic conductance  $\sigma_V$  and the same metrics. The top row (A) shows COS, the middle row (B) shows ISI Density ( $ms^{-1}$ ), and the bottom row (C) shows SNR\* ( $mV^{-1}$ ). Filled circles and solid lines represent  $ISI = 100\ ms, c = 0.7$ . Open circles and dashed lines represent  $ISI = 200\ ms, c = 0.7$ .

$\Delta v_e =$

Figure 3. Characteristic curves of the model for  $c = 0.7$ . The left column shows the relationship between the adjusted synaptic conductance  $a_{adj\ sc}$  and the metrics COS, ISI Density, and SNR\*. The right column shows the relationship between the standard deviation of the synaptic conductance  $\sigma_V$  and the same metrics. The top row (A) shows COS, the middle row (B) shows ISI Density ( $ms^{-1}$ ), and the bottom row (C) shows SNR\* ( $mV^{-1}$ ). Filled circles and solid lines represent  $ISI = 100\ ms, c = 0.7$ . Open circles and dashed lines represent  $ISI = 200\ ms, c = 0.7$ .

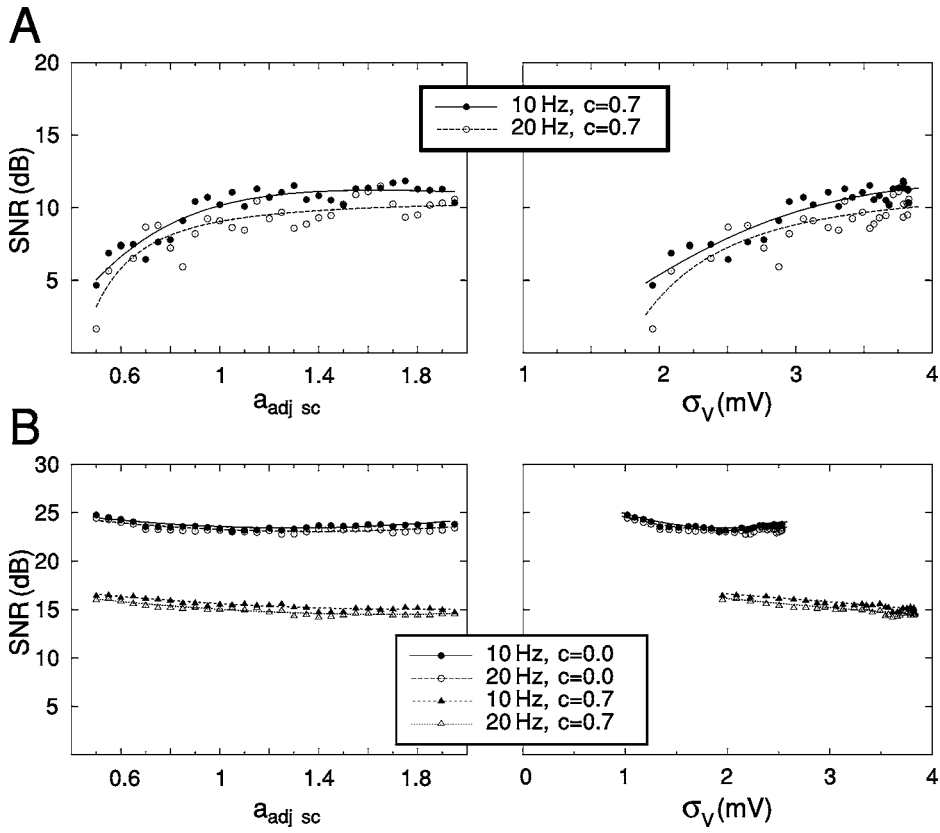


Figure 4. SNR vs.  $a_{adj\ sc}$  and  $\sigma_V$  for different frequencies and correlation coefficients.

A:  $c = 0.7$

B:  $c = 0.0$  d  $c = 0.7$

$V_m$

$\sigma_V$

$c = 0.0$  d  $c = 0.7$ . A:  $c = 0.7$

$V_m$

$\sigma_V$

$V_m$

$\sigma_V$

$V_m$

$\sigma_V$

$V_m$

$\sigma_V$

$V_m$

$\sigma_V$

$V_m$

$\sigma_V$

$V_m$

$\sigma_V$

$V_m$

$\sigma_V$

$V_m$

$\sigma_V$

$V_m$

$\sigma_V$

$V_m$

$\sigma_V$

$V_m$

$\sigma_V$

$V_m$

$\sigma_V$

$V_m$

$\sigma_V$

$V_m$

$\sigma_V$

$V_m$

$\sigma_V$

$V_m$

$\sigma_V$

$V_m$

$\sigma_V$

$V_m$

$V_m$

$c = 0.7$

$V_m$

$\sigma_V$

$V_m$

$\sigma_V$

$V_m$

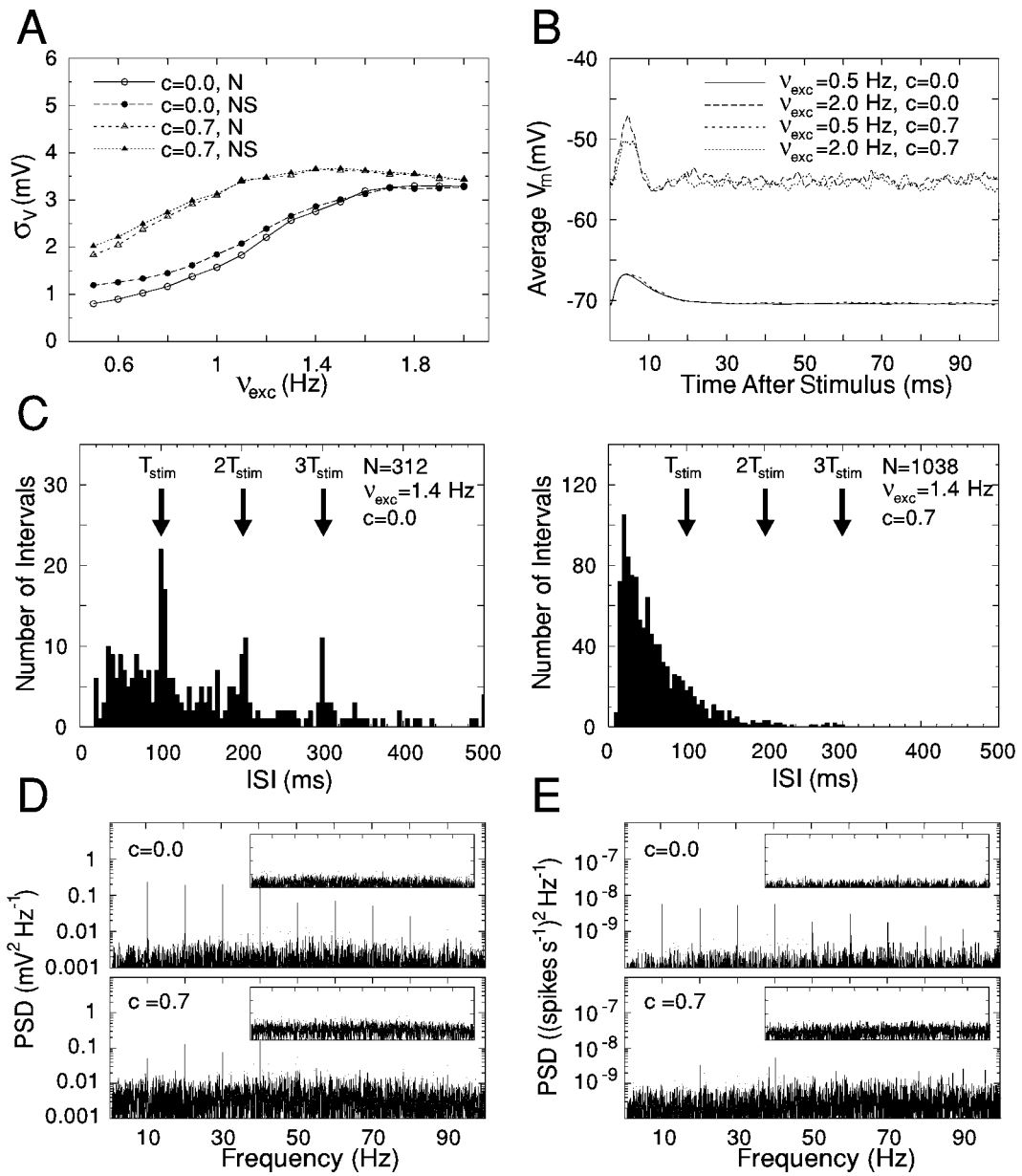


Figure 5. **A:** Plot of the standard deviation of the membrane potential,  $\sigma_V$ , versus the excitation frequency,  $\nu_{exc}$ , for different coupling strengths,  $c$ , and noise levels,  $N$  (solid lines) and  $NS$  (dashed lines). **B:** Average membrane potential,  $V_m$ , versus time after stimulus for different excitation frequencies,  $\nu_{exc}$ , and coupling strengths,  $c$ . **C:** Histograms of interspike intervals (ISI) for  $N=312$  ( $c=0.0$ ) and  $N=1038$  ( $c=0.7$ ) at  $\nu_{exc}=1.4$  Hz. **D** and **E:** Power Spectral Density (PSD) versus Frequency (Hz) for  $c=0.0$  and  $c=0.7$ , respectively.

Figure 6 (continued)  
 (Fig 5D-E) with  
 $c = 0.7$ .  
 $v_e$ ,  $\delta V_m$   
 $\nu_e$ ,  $\delta V_m$

$c = 0.7$ .

$v_e$   $\delta V_m$

Figure 6 (continued)  
 (Fig 6 d).  
 $\nu_e$ ,  $\delta V_m$   
 $\nu_e$ ,  $\delta V_m$

$\nu_e$

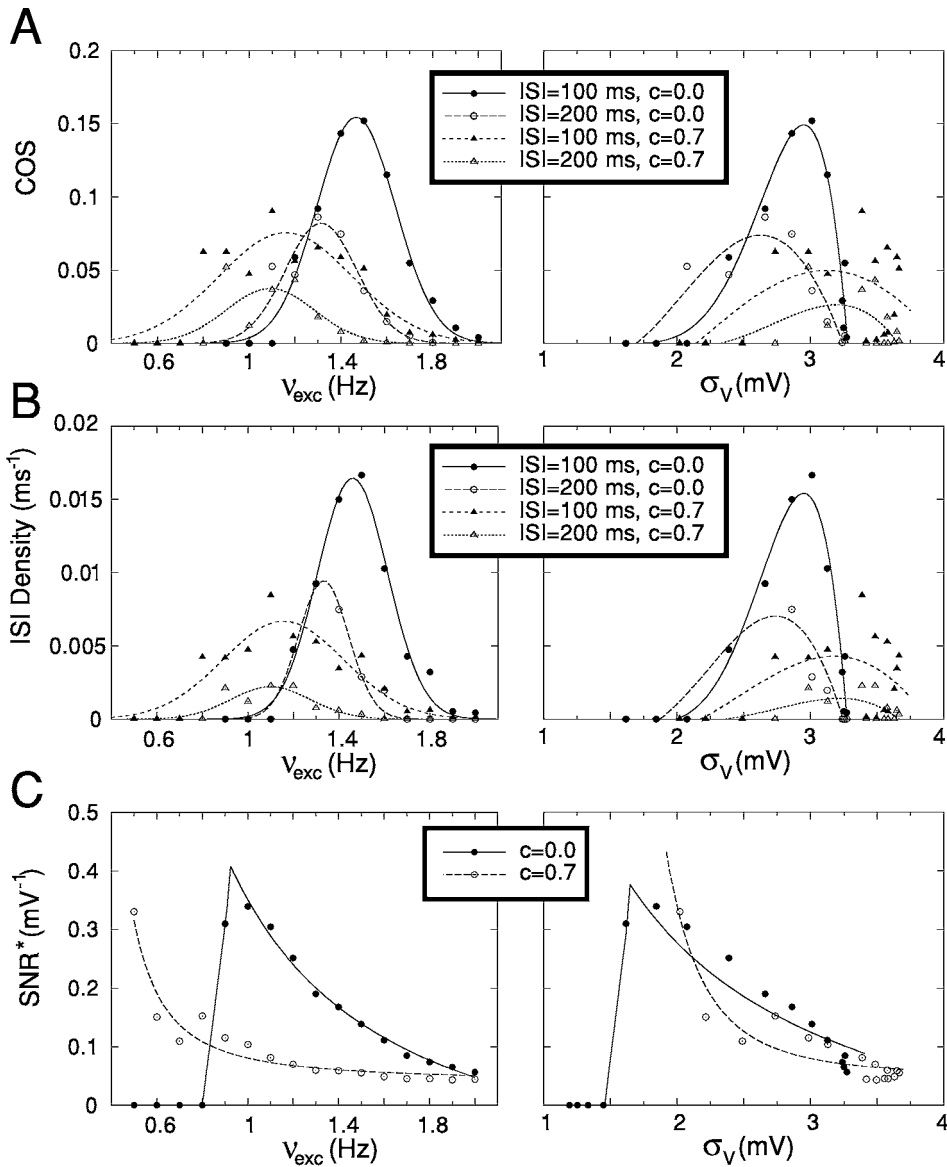


Figure 6. COS vs  $V_{exc}$  (Hz) and  $\sigma_V$  (mV) for different ISI and  $c$  values. The y-axis is COS, the x-axis is  $V_{exc}$  (Hz) and  $\sigma_V$  (mV). The legend indicates four data series: ISI=100 ms, c=0.0 (solid line, filled circles); ISI=200 ms, c=0.0 (dashed line, open circles); ISI=100 ms, c=0.7 (dotted line, filled triangles); ISI=200 ms, c=0.7 (dash-dot line, open triangles).

$\nu_e$ ,  $\delta V_m$

B: D for 100 and 200 ms

C: SNR\* vs  $V_{exc}$  (Hz) and  $\sigma_V$  (mV)



$\sigma_V \sim 1.7 V_m$   
 $c = 0.0$  (Fig 7A).  
 $V_m$

(Fig 8A), Fig 8B  
 $V_m$   
 $\leq \sigma_V \leq 7.5 M$   
 $.5 M \leq \sigma_V \leq 6.5 M$   
 $\leq \sigma_V \leq 5.5 M$   
 $\sigma_V \sim 0.5 M$   
 $c$   
 $\sigma_V$   
 $c \sim 0.65$   
 $V_m$

3.3. Correlation Study: The Impact of the Background Statistics

(e.g. Duf  
 1999),  
 $V_m$   
 $c$   
 $\Delta c = 0.05$  if  $c \leq 0.90$   
 $\Delta c = 0.01$  if  $c > 0.90$ .  
 $a_c = 0.7$  if  $a_c = 1.0$ .  
 $V_m$   
 $c \sim 0.9$ ,  $V_m$   
 $-65$   
 $c$ .  
 $V_m$

$\epsilon$   
 $V_m$   
 Fig 8C.  
 $c$ .  
 (Fig 8D eE)  
 $V_m$   
 $c$ .  
 $V_m$

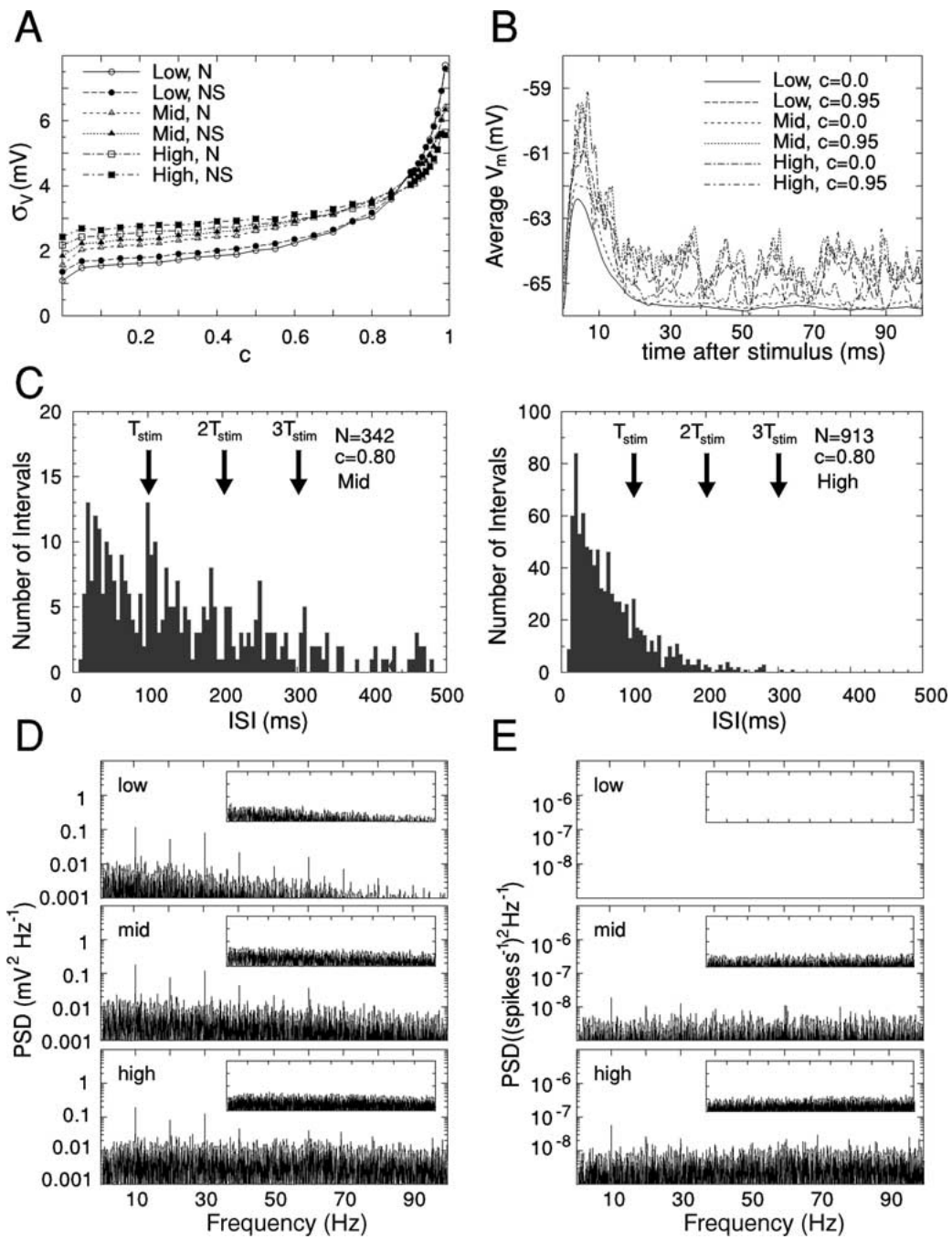


Figure 8. **A:**  $\sigma_V$  vs.  $c$  for different firing rates and noise levels. **B:** Average  $V_m$  vs. time after stimulus for different firing rates and noise levels. **C:** Histograms of interspike intervals (ISI) for mid and high firing rates. **D:** Power spectral density (PSD) vs. frequency for low, mid, and high firing rates. **E:** PSD vs. frequency for low, mid, and high firing rates with a logarithmic y-axis.

**A:**  $\sigma_V$  vs.  $c$  for different firing rates and noise levels. **B:** Average  $V_m$  vs. time after stimulus for different firing rates and noise levels. **C:** Histograms of interspike intervals (ISI) for mid and high firing rates. **D:** Power spectral density (PSD) vs. frequency for low, mid, and high firing rates. **E:** PSD vs. frequency for low, mid, and high firing rates with a logarithmic y-axis.



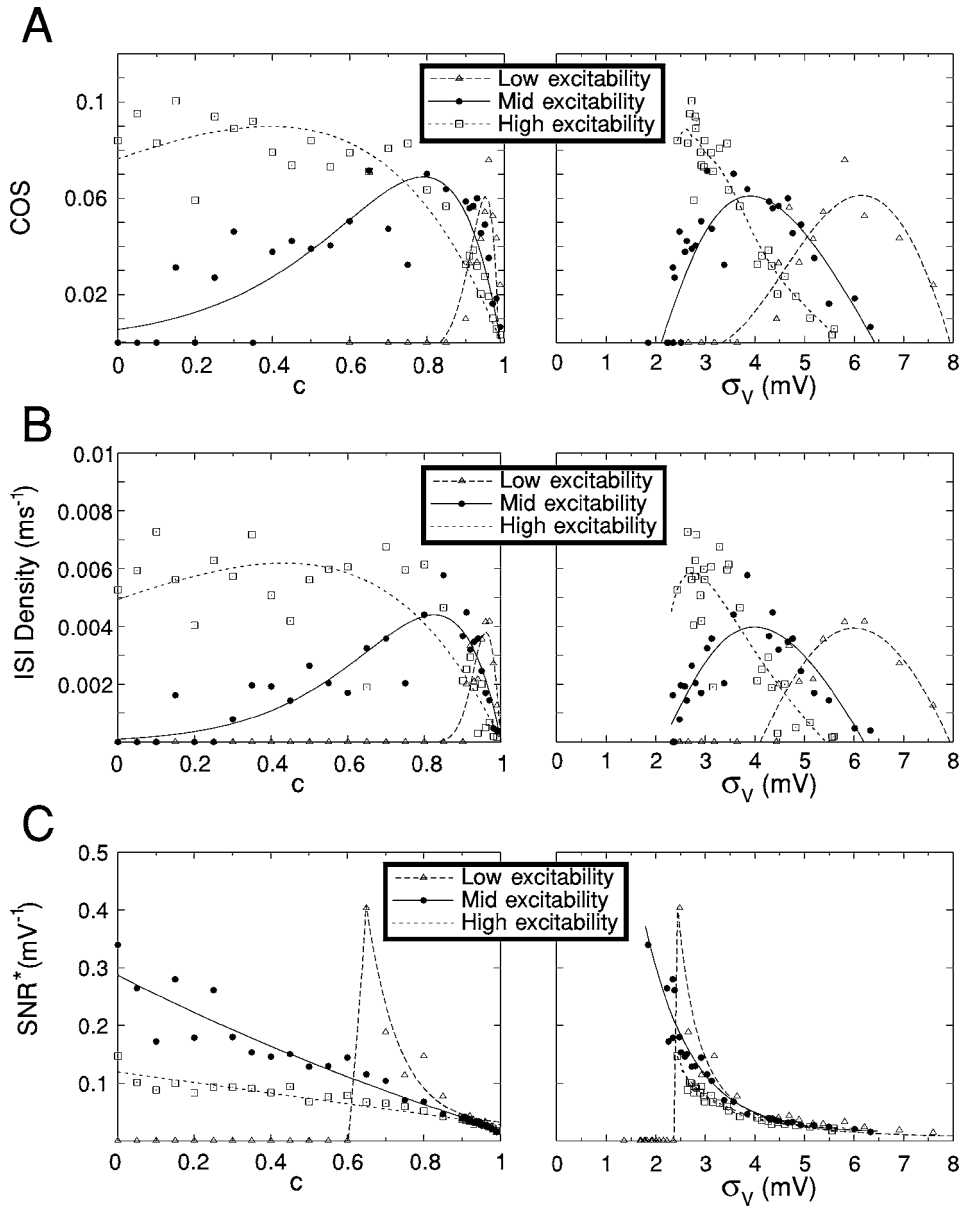


Figure 9. Relationship between excitability levels and various metrics.

Fig 9 d10

$c$

$\sigma_V$

C:  $\text{SNR}^*$

$c$

$\sigma_V$

$\sigma_V \sim 6$

$c \sim 0.95$   
 $c \sim 0.75$

$\sigma_V$

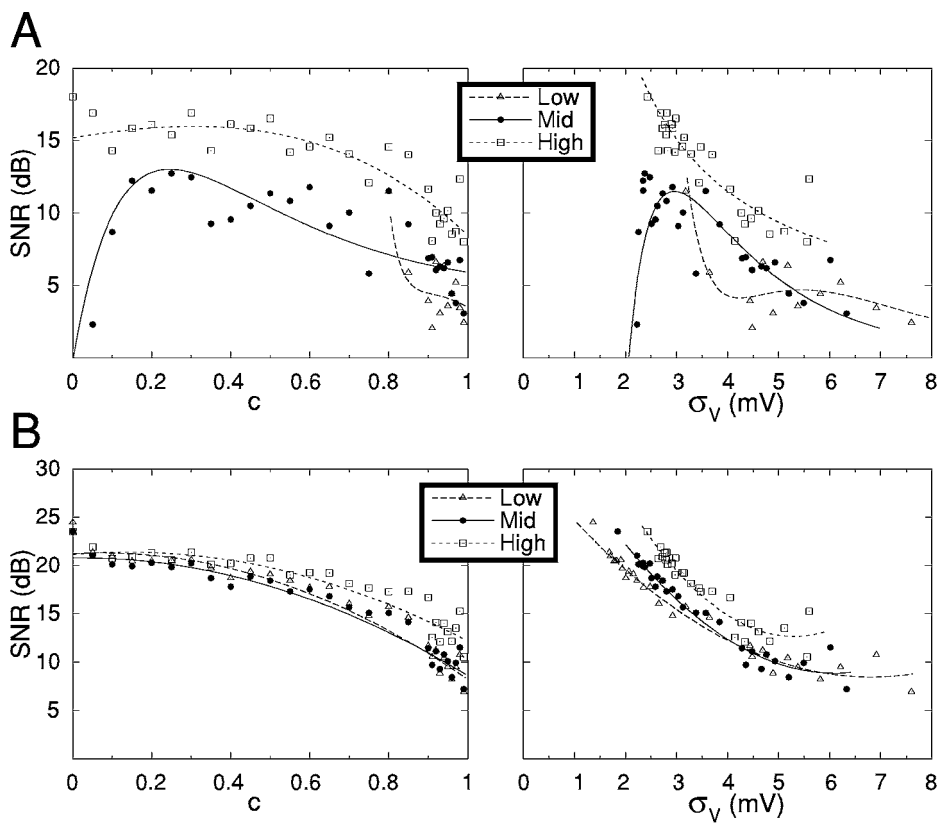


Figure 10. SNR vs  $c$  and  $\sigma_V$ .

A: SNR vs  $c$  (left) and  $\sigma_V$  (right).  
 B: SNR vs  $c$  (left) and  $\sigma_V$  (right).

Legend: Low (dashed line, triangles), Mid (solid line, circles), High (dotted line, squares).

$V_m$  (mV)

$\sigma_V$  (mV)

SNR (dB)  
 $c$   
 $V_m$  (mV)  
 $\sigma_V$  (mV)

$c$

$\sigma_V$

SNR (dB)  
 $\sigma_V$  (mV)  
 $c \sim 0.6, \sigma_V \sim 2.5$  M  
 Fg10C).  
 \* As  
 \*  
 Fg10B)

3.4. Robustness of Stochastic Resonance-Like Behavior

$\Delta V$  fidelity  
 gabapentin  
 it  
 d  
 y(c) v  
 R  
 p  
 $I_K$ , d  $I_M$  a Ca  
 p(C-  
 h, 1989)

(1992)  
 2 M  
 C  
 (Fig 11A),  
 $Ca^{2+}$   
 $I_N$ ,  
 $I_{Ca^{2+}}$   
 (1999)

$I_{Ca}$   
 $V_m$   
 $\leq \sigma_V \leq 11$

$\sigma_V \sim 6$

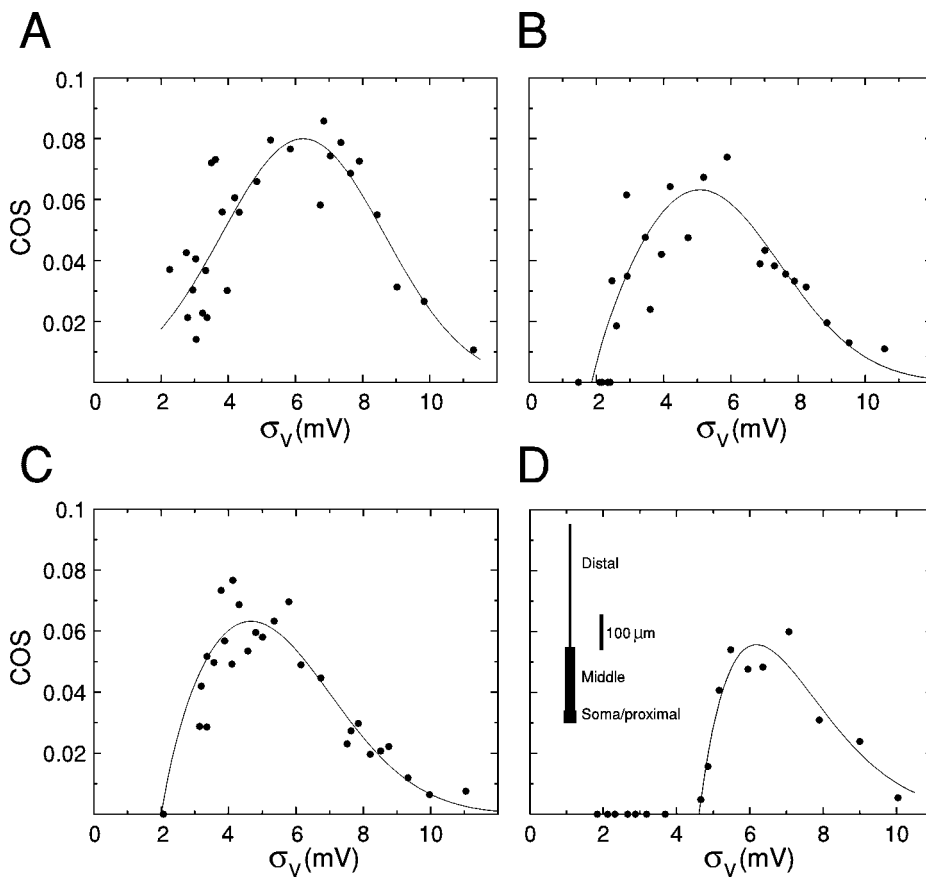


Figure 11. A: AHCa  $I_N$ ,  $I_K$ , d  $I_M$   $\sigma_V \sim 6$   
 B:  $I_{Ca^{2+}}$   
 C:  $I_{Ca^{2+}}$   
 D: A  $I_K$   $V_m$

the standard deviation  $\sigma_V$  is

$$.5 M \leq \sigma_V \leq 12 M$$

(Fig 11B). The standard deviation  $\sigma_V \sim 5 M$  (Fig 11C).

(Fitz, 1990; Destexhe, 1992) (Fig 11C).

$$I_N, I_K, I_M, V_m, V_m$$

the standard deviation  $\sigma_V \sim 6 M$

#### 4. Discussion

the standard deviation  $\sigma_V \sim 6 M$

the standard deviation  $\sigma_V \sim 6 M$

##### 4.1. Measures of Response Coherence and Their Applicability

the standard deviation  $\sigma_V \sim 6 M$

the standard deviation  $\sigma_V \sim 6 M$

the standard deviation  $\sigma_V \sim 6 M$

the standard deviation  $\sigma_V \sim 6 M$

the standard deviation  $\sigma_V \sim 6 M$

the standard deviation  $\sigma_V \sim 6 M$

the standard deviation  $\sigma_V \sim 6 M$

the standard deviation  $\sigma_V \sim 6 M$

the standard deviation  $\sigma_V \sim 6 M$

the standard deviation  $\sigma_V \sim 6 M$

the standard deviation  $\sigma_V \sim 6 M$

the standard deviation  $\sigma_V \sim 6 M$

the standard deviation  $\sigma_V \sim 6 M$

the standard deviation  $\sigma_V \sim 6 M$

the standard deviation  $\sigma_V \sim 6 M$

the standard deviation  $\sigma_V \sim 6 M$

the standard deviation  $\sigma_V \sim 6 M$

the standard deviation  $\sigma_V \sim 6 M$

the standard deviation  $\sigma_V \sim 6 M$

the standard deviation  $\sigma_V \sim 6 M$

the standard deviation  $\sigma_V \sim 6 M$

the standard deviation  $\sigma_V \sim 6 M$

the standard deviation  $\sigma_V \sim 6 M$

the standard deviation  $\sigma_V \sim 6 M$

the standard deviation  $\sigma_V \sim 6 M$

the standard deviation  $\sigma_V \sim 6 M$

the standard deviation  $\sigma_V \sim 6 M$

(Bich, 1981; Foch, 1993; Gershenson, 1991).

Figure 3A shows the membrane potential  $V_m$  (Fig 2B). For  $c = 0.0$  (Fig 5A), and  $c = 0.7$  (Fig 6A-B). The membrane potential  $V_m$  (Fig 4B).

Figure 7A shows the membrane potential  $V_m$  (Fig 7A). For  $c = 0.7$  (Fig 7B).

Figure 8A shows the membrane potential  $V_m$  (Fig 8A-B). For  $c = 0.0$  (Fig 8A) and  $c = 0.7$  (Fig 8B). The membrane potential  $V_m$  (Fig 8A-B).

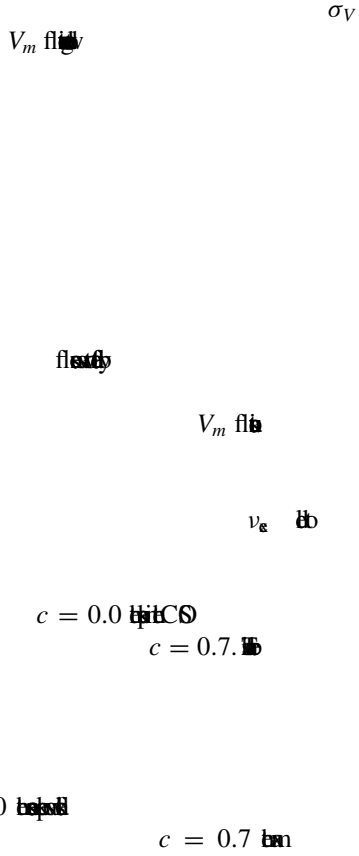


Figure 4: Membrane potential  $V_m$  vs time for different values of  $\sigma_V$ . The plot shows  $V_m$  on the y-axis and time on the x-axis. Two traces are shown: one for  $\sigma_V = 0.5$  and one for  $\sigma_V = 4$ . The  $\sigma_V = 0.5$  trace shows a regular oscillation, while the  $\sigma_V = 4$  trace shows a more irregular, noisy oscillation.

4.3. "Nonclassical" Stochastic Resonance

A nonclassical stochastic resonance is observed when the noise intensity  $\sigma_V$  is tuned to match the system's natural frequency. This is shown in Figure 5 (Fig 5A, B) and Figure 6 (Fig 6A, B).

Figure 7 (Fig 7A, B) shows the membrane potential  $V_m$  for different values of  $\sigma_V$  and  $c$ . The plot shows  $V_m$  on the y-axis and time on the x-axis. Two traces are shown: one for  $\sigma_V = 0.5$  and one for  $\sigma_V = 4$ . The  $\sigma_V = 0.5$  trace shows a regular oscillation, while the  $\sigma_V = 4$  trace shows a more irregular, noisy oscillation.

Figure 8 (Fig 8A, B) shows the membrane potential  $V_m$  for different values of  $\sigma_V$  and  $c$ . The plot shows  $V_m$  on the y-axis and time on the x-axis. Two traces are shown: one for  $\sigma_V = 0.5$  and one for  $\sigma_V = 4$ . The  $\sigma_V = 0.5$  trace shows a regular oscillation, while the  $\sigma_V = 4$  trace shows a more irregular, noisy oscillation.

Figure 9 (Fig 9A, B) shows the membrane potential  $V_m$  for different values of  $\sigma_V$  and  $c$ . The plot shows  $V_m$  on the y-axis and time on the x-axis. Two traces are shown: one for  $\sigma_V = 0.5$  and one for  $\sigma_V = 4$ . The  $\sigma_V = 0.5$  trace shows a regular oscillation, while the  $\sigma_V = 4$  trace shows a more irregular, noisy oscillation.

Figure 10 (Fig 10A, B) shows the membrane potential  $V_m$  for different values of  $\sigma_V$  and  $c$ . The plot shows  $V_m$  on the y-axis and time on the x-axis. Two traces are shown: one for  $\sigma_V = 0.5$  and one for  $\sigma_V = 4$ . The  $\sigma_V = 0.5$  trace shows a regular oscillation, while the  $\sigma_V = 4$  trace shows a more irregular, noisy oscillation.

4.4. Possible Functional Consequences

The results suggest that stochastic resonance can be used to enhance the signal-to-noise ratio in a system. This is shown in Figure 11 (Fig 11A, B) and Figure 12 (Fig 12A, B).



CHEN (1996) *J. Neurophysiol.* 76:642–645.

CHEN, D. & H. (1997) *J. Neurophysiol.* 78:335–350.

CHEN, H. & H. (1996) *J. Physiol.* 494:251–264.

CHEN, D. (1997) *J. Neurophysiol.* 78:2116–2128.

CHEN (1967) *J. Anat.* 101:639–654.

DE J. F. (1992) *Prog. Neurobiol.* 39:563–607.

D. (1989) *Phys. Rev. Lett.* 63:207–210.

D. & H. (1998) *Methods in Neuronal Modeling (2nd ed.)* 26.

D. (2001) *Neurocomputing.* 38:167–173.

D. & P. (1999) *J. Neurophysiol.* 81:1531–1547.

D. & H. (1993) *Nature* 365:337–340.

E. (1964) *J. Neurophysiol.* 27:152–171.

F. (1993) *Phys. Lett.* A97:5–7.

F. & H. (1990) *J. Gen. Physiol.* 95:1139–1157.

H. (1998) *Rev. Mod. Phys.* 70:223–287.

H. & A. (1989) *IEEE Trans. Biomed. Eng.* 36:4–14.

H. & K. (1974) *J. Comp. Neurol.* 154:1–27.

H. (1997) *Neural Computation* 9:1179–1209.

H. (2000) *J. Neurophysiol.* 84:1488–1496.

H. & F. (1952) *J. Physiol.* 117:500–544.

H. (1959) *J. Physiol.* 147:226–238.

H. & D. (1998) *BioSystems* 48:95–104.

H. & D. (1988) *J. Neurophysiol.* 59:778–795.

H. & D. (1992) *J. Neurophysiol.* 68:1373–1383.

H. & A. (1998) *J. Neurophysiol.* 79:1879–1890.

H. & K. (1998) *Nature Neuroscience* 1:384–388.

H. & C. (1996) *Annual Rev. Neurosci.* 19:165–186.

H. & F. (1999) *Neuron* 22:361–374.

H. & A. (1991) *J. Comp. Neurol.* 306:332–343.

H. (1999) *Phys. Rev. E* 60:826–830.

H. & K. (1998) *Phys. Rev. E* 57:3292–3297.

H. & H. (1996) *Nature* 380:165–168.

H. (1993) *J. Stat. Phys.* 70:309–327.

H. & B. (1991) *Phys. Rev. Lett.* 67:656–659.

H. & C. (1998) *Phys. Rev. Lett.* 81:4012–4015.

H. (1996) *Neural Computation* 8:501–509.

H. & H. (1995) *J. Physiol.* 487:67–90.

H. & H. (1995) *Science* 268:301–304.

H. & C. (1999) *Proc. Natl. Acad. Sci. USA* 96:10450–10455.

H. (1998) *Phys. Rev. E* 58:876–880.

H. & F. (1988) *Exp. Brain Res.* 70:463–469.

H. & H. (1992) *J. Neurophysiol.* 68:1384–1400.

H. & H. (1999) *J. Comp. Neurosci.* 7:5–15.

BA, BAO, BAW, Bn  
 H, BAK(1999) *Phys*  
 663. *Phys. Rev. Lett.* 82:660–663.

BA, BEL, BF, GB, CbJ  
 (1999) *Phys*  
*Phys. Rev. E* 60:284–292.

BK (1982) *Tellus* 34:1.

BSM, BDA (1997) *in*  
*Cereb. Cortex* 7:487–501.

B ED, BE, BHD, BJA, BEJ(1998) *in*  
*J. Neurophysiol.* 79:1450–1460.

BKL, BNT (1996) *in*  
*J. Neurophysiol.* 76:3002–3011.

BWA, BVB, BR(1993) *Nu-*  
*merical Recipes in C: The Art of Scientific Computing.* (2nd).

BWC, BJC(1998) *in*  
*Chaos* 8:599–603.

BMD, BA (2000) *Soc. Neurosci. Abstracts*  
 26:1623.

BK, RW(1998) *Trends*  
*Neurosci.* 21:453–460.

BBA, BBR(1999) *Phys. Rev. E* 59:3461–3470.

BE, BMS, BML, BF  
 (1997) *Phys. Rev. Lett.*  
 78:1186–1189.

BR, BR(1999) *Phys. Rev. E* 59:2566–2570.

BW, DDM(2000) *J. Neurophysiol.*  
 83:1394–1402.

BV(1978) *Behav. Brain Sci.* 3:465–514.

BWF (2001) *J. Neurophysiol.*  
 85:1969–1985.

BCB (1994) *Nature*  
 367:69–72.

B (1965) *Progress*  
*in Brain Research* 14. E:1–32.

BB, B(1991) *Neuronal Networks of the Hippocampus.*

BWC, BJC  
 (1998) *Phys. Rev. E* 57:R527–R530.

BML(1989) *Cortical Circuits.* B:1–36.

BBI (1995) *Nature* 373:33–36.

BWC, ABR(1989) *Methods in Neuronal*  
*Modeling.* B:1–14.

BBI (1990) *Phys. Rev.* A41:4255–4264.

BE, BMM(1994) *Nature* 370:140–143.